

# Diagnosis of Frequency Response Analog Circuits using HHO-SVM

R. Gurunadha<sup>1,\*</sup>, Dr. K. Babulu<sup>2</sup>

<sup>1</sup> Associate Prof, Department of ECE, JNTUGV-CEV, Vizianagaram India;

<sup>2</sup> Professor, Department of ECE, JNTUGV-CEV, Vizianagaram, India

\*Correspondence: gururavva@gmail.com

**Abstract-** Monitoring the system, recognising when a fault has occurred, identifying the kind of defect and where it is located are all aspects of fault detection and isolation. To assess whether a problem has arisen inside a certain channel or region of operation, fault detection is used. For many technological processes in the creation of effective and safe advanced supervision systems, fault detection and diagnosis have grown in significance. This article's main goal is to increase the accuracy of faults detection in frequency response analogue circuits and execution of work needs to be speed up. For this purpose, two optimization techniques are used. One is grey wolf optimization (GWO) for the process of feature extraction and secondly Harris Hawk optimization (HHO) as classifier optimizer. the features and optimize the classifier. The Sallen key circuit (SKC) are utilized for processing the input data. The filters like low pass, high pass and bandpass are designed based on SKC and optimized using GWO. Finally, the optimized features obtained from different circuits are fed to support vector machine classifier to identify the fault accuracy in the circuit. The SVM classifier is optimized using HHO to achieve best accurate output. The suggested technique with a low-dimensional feature optimisation and optimised classifier performed better than the prior methods according to simulation findings, and computing time was also greatly minimised.

**Keywords-** Analogue circuits, Sallen key circuit, GWO, HHO, SVM.

## 1. Introduction

Analogue integrated circuits are employed in a variety of fields, including as measurement, control, and communication systems. Analogue circuits may be more challenging to identify and diagnose flaws in due to their high level of intricacy and variation. Conventional methodologies for detection of faults in analogue circuits, such as analysis of signature and modelling of circuit are limited in their accuracy, speed, and scalability.

On analogue circuits, the performance-related impacts of different fault types have a considerable impact. The two types of flaws are catastrophic faults and parametric faults. Catastrophic errors result in the circuit's total inability to function. These include ground faults, which occur when a signal or element has been connected to ground, short circuit faults, which occur when component pins or conducting channels come into contact with one another. The circuit might malfunction or fail as a result of these defects. On the other hand, parametric mistakes result in the circuit behaving inconsistently or producing inaccurate output. These include issues with the supply of power such as overvoltage or undervoltage situations, thermal drift brought on by changes in component temperatures, and noise brought on by undesirable interference of signal.

Due to their extensive use in many electronic systems, analogue circuits' skills for fault categorization and problem detection have assumed increased significance. Due to its ability to handle massive amounts of data and precisely categorise errors, machine learning (ML) approaches have gained popularity in recent years for the purpose of

identifying and categorising defects in analogue circuits. The fault detection method utilised for this function combines data from many sources to increase accuracy. This method is based on a multi-source data fusion-based parametric fault diagnosis approach for analogue circuits that was developed in [1]. The method estimates an analogue circuit's parameters and looks for errors using an enhanced Kalman filter. The authors in [2–3] described a method for classifying analogue defects based on adaptive neuro-fuzzy and reduction of features. The classifier can accurately classify issues by just considering the essential factors.

There have been other methods proposed for the detection and diagnosis of analogue errors, including analysis of impulse response [4], Traits of frequency response [5], and digital testing techniques based on frequency band categorization and effective test-point selection [6]. The DC testing method has been used to find and identify both open and hard defects [7-8]. The proposed methodology is also intended to diagnose these faults concurrently, as opposed to other prior techniques that were used to detect different soft faults that occur in linear analogue circuits. Thus, it has successfully served as a diagnostic tool for intricate analogue circuits [9].

An effective and precise classifier is initially a key component in classification of faults. The statistical learning theory-based support vector machine (SVM) [10] offers the benefits of a straightforward construction, an approachable theoretical foundation, and a training a sample size which is small. For binary and multivariate classification, SVM, a supervised learning technique splits features in the feature space to identify separation hyperplanes and using kernel

functions, it may also address non-linear classification problems. SVM is frequently employed to address classification issues. The kernel function and penalty settings of the SVM have a significant influence on the accuracy of the classification performed [11]. For the tuning of these parameters, cross-grid validation is frequently utilised. The best grid to find each node is created via linear gridding. Grid resolution and vector space have an impact on the process time and outcomes of optimisation. Training takes a very long time because of how inefficient the optimisation is.

There is no one optimal metaheuristic algorithm to address all optimisation problems, as demonstrated by the "No Free Lunch" theorems (NFL) put out by the author in [15], which stimulated the development of new optimisation algorithms. The genetic algorithm (GA) [12], particle swarm optimisation (PSO) [13], and the ant lion optimisation algorithm (ALO) [14] are some examples of these algorithms. The barnacles matching optimizer (BMO), a brand-new biological population metaheuristic intelligence method, was presented in [16].

How to apply the optimisation approach to develop a classifier that is both efficient and accurate is another topic that requires exploration. Second, the feature extraction method employed for soft fault detection of analogue circuits has a direct influence on the accuracy of classification. A substantial connection between the fault features and the fault-free features as well as between different fault features may exist when the traits of fault elements vary over a wide range, especially when the permissible tolerance of every element is taken into account, making classification

challenging. To generate a large amount of data while simultaneously making sure the data is as complete as is practical, the feature vectors produced by general simulation are relatively large in size. Another problem worth investigating is how to efficiently extract, filter, and categorise feature vectors and fault excitation vectors.

In order to overcome the two difficulties described above, the following have been used in this study: It is advised to use an improved grey wolf optimizer (IGWO), which has accelerated convergence speed, exploration capabilities, and jump-out capabilities, to extract the features. The performance is assessed using four different test circuits. The SVM classifier based on Harris Hawks Optimisation (HHO) is proven in both its design and performance. It develops a method for identifying problems in analogue circuits. To address the analogue circuit component parameter problem broad range dispersion diagnostics for tolerance and fault parameters, the convergence of various faults was simulated using the Matlab software tool.

**2. Circuits for Testing**

The circuits considered for testing are of four different types. One is the Sallen–Key low pass circuit (SK-LPC) which is shown in in fig 1(a). The second circuit is Sallen–Key high pass circuit (SK-HPC) which is shown in fig 1(b). The third is Sallen–Key band pass circuit (SK-BPC) which is shown in fig. 2. Finally, the fourth is Sallen–Key band stop circuit (SK-BSC) which is shown in fig. 3. 10% of the nominal value is the normal tolerance range of the components in resistors and capacitors.

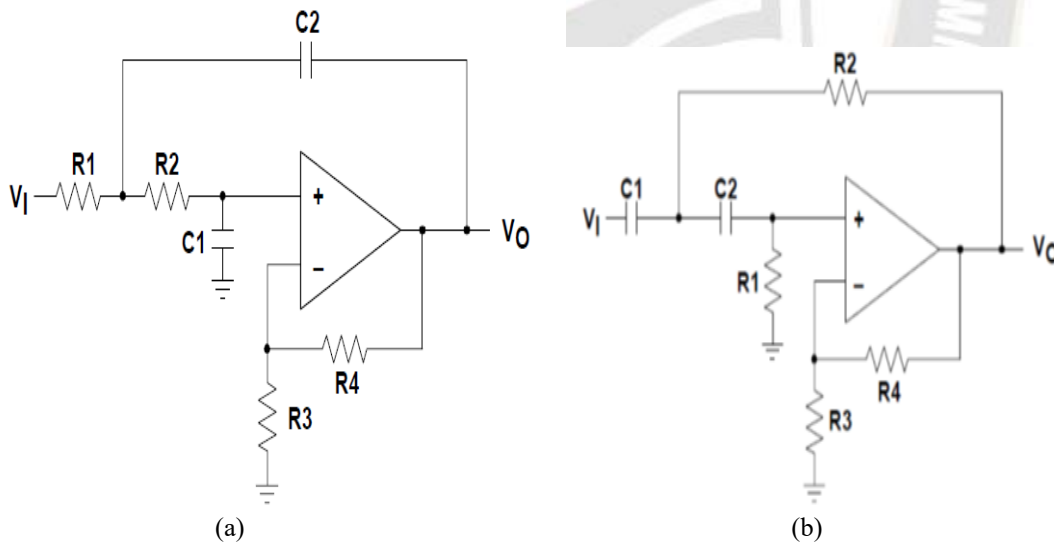


**Fig. 1 Sallen Key (a) LPC (b) HPC**

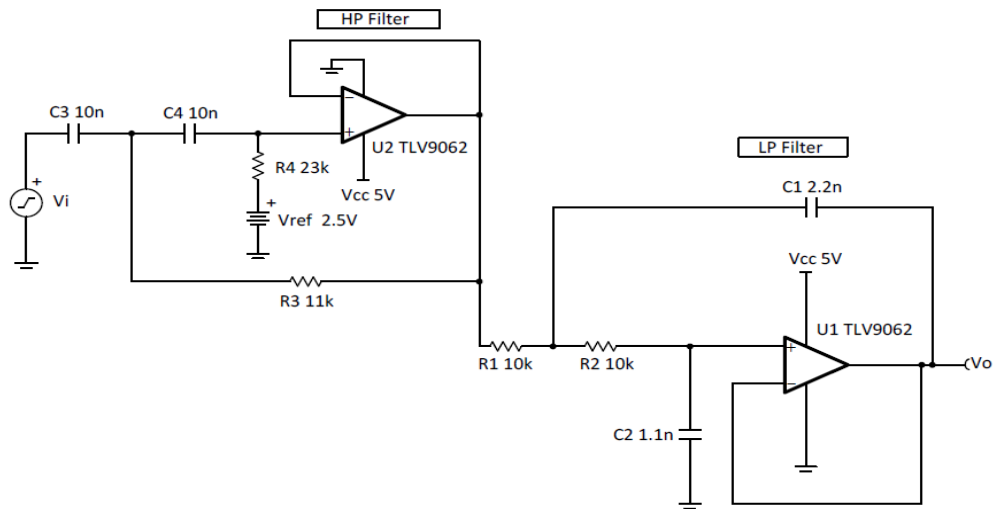


**Fig. 2 SK-BPC for test**

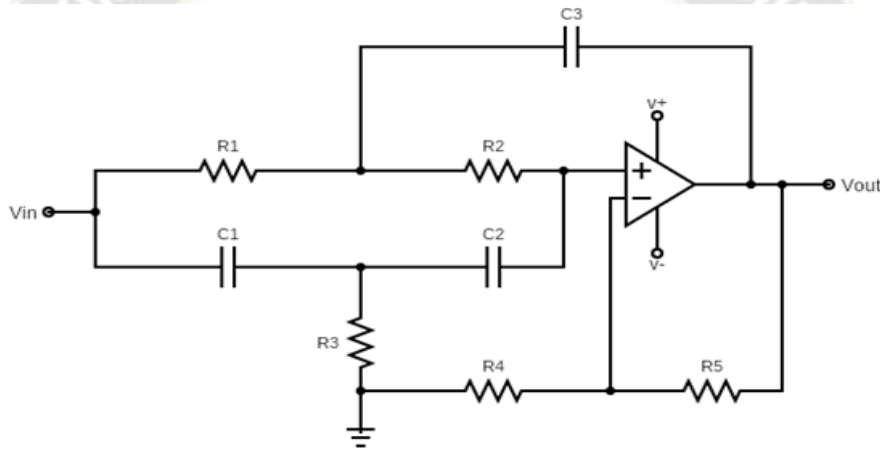


**Fig. 3 SK-SBC for test**

Tables 1, 2, 3, and 4 include the elements' nominal values as well as their incorrect values. As previously, 10% is regarded as the accepted standard tolerance for the elements for capacitors and resistance. The fault classes that are taken into

consideration are still separated into the defective class and the fault-free class. In the four circuits under test (CUTs) that are being studied, faults are produced by varying the values of capacitors and resistors.

**Table 1. Nominal and faulty values for SK-LPC**

Fault Code	Fault Class	Nominal Value	Fault Value
F0	NF	.....	.....
F1	C1↑	1nF	2nF
F2	C1↓	1nF	0.5nF
F3	C2↑	1nF	2nF
F4	C2↓	1nF	0.5nF
F5	R1↑	1kΩ	2kΩ
F6	R1↓	1kΩ	0.5kΩ
F7	R2↑	1kΩ	2kΩ
F8	R2↓	1kΩ	0.5kΩ
F9	R3↑	2kΩ	3kΩ
F10	R3↓	2kΩ	0.5kΩ
F11	R4↑	1kΩ	2kΩ
F12	R4↓	1kΩ	0.5kΩ

**Table 2. Nominal and faulty values for SK-HPC**

Fault Code	Fault Class	Nominal Value	Fault Value
F0	NF	.....	.....
F1	C1↑	1nF	1.5nF
F2	C1↓	1nF	0.8nF
F3	C2↑	1nF	1.4nF
F4	C2↓	1nF	0.86nF
F5	R1↑	1kΩ	1.45kΩ
F6	R1↓	1kΩ	0.54kΩ
F7	R2↑	1kΩ	1.5kΩ
F8	R2↓	1kΩ	0.75kΩ
F9	R3↑	2kΩ	2.3kΩ
F10	R3↓	2kΩ	1.6kΩ
F11	R4↑	1kΩ	1.7kΩ
F12	R4↓	1kΩ	0.8kΩ

**Table 3. Nominal and faulty values for SK-BPC**

Fault Code	Fault Class	Nominal Value	Fault Value
F0	NF	.....	.....
F1	C1↑	2.2nF	2.5nF
F2	C1↓	2.2nF	2nF
F3	C2↑	1.1nF	1.4nF
F4	C2↓	1.1nF	0.8nF
F5	C3↑	10nF	11.2nF
F6	C3↓	10nF	9.6nF
F7	C4↑	10nF	10.35nF
F8	C4↓	10nF	9.75nF
F9	R1↑	10kΩ	10.4kΩ
F10	R1↓	10kΩ	9.72kΩ
F11	R2↑	10kΩ	10.31kΩ
F12	R2↓	10kΩ	9.82kΩ
F13	R3↑	11kΩ	11.5kΩ
F14	R3↓	11kΩ	10.7kΩ
F15	R4↑	23kΩ	23.7kΩ
F16	R4↓	23kΩ	22.6kΩ

**Table 4. Nominal and faulty values for SK-BSC**

Fault Code	Fault Class	Nominal Value	Fault Value
F0	NF	.....	.....
F1	C1↑	2.2nF	2.6nF
F2	C1↓	2.2nF	1.8nF
F3	C2↑	1.1nF	1.5nF
F4	C2↓	1.1nF	0.76nF
F5	C3↑	10nF	11.35nF
F6	C3↓	10nF	9.5nF
F7	R1↑	10kΩ	10.5kΩ
F8	R1↓	10kΩ	9.6kΩ
F9	R2↑	10kΩ	10.45kΩ

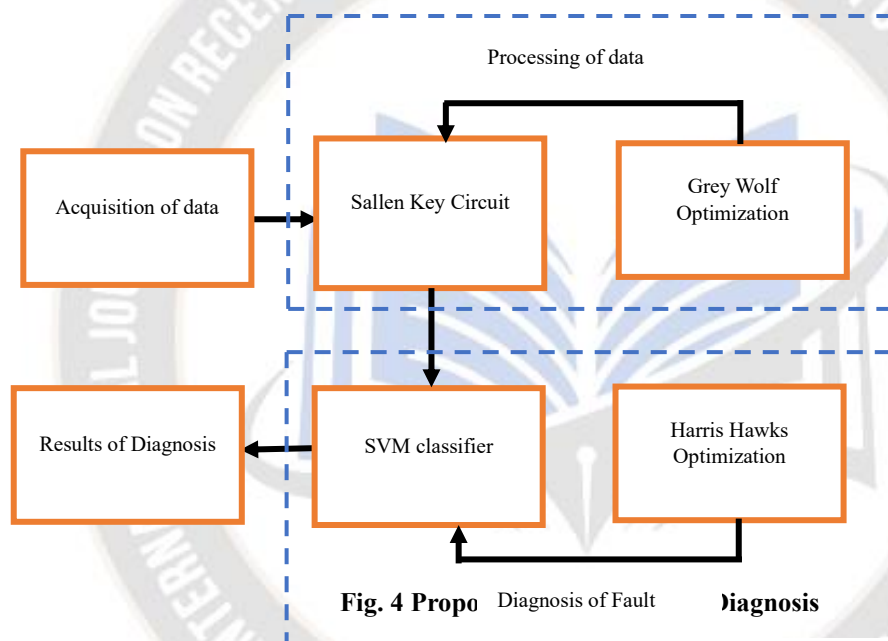


F10	R2↓	10kΩ	9.6kΩ
F11	R3↑	10kΩ	10.8kΩ
F12	R3↓	10kΩ	9.5kΩ
F13	R4↑	10kΩ	10.8kΩ
F14	R4↓	10kΩ	9.2kΩ
F15	R5↑	10kΩ	10.7kΩ
F16	R5↓	10kΩ	9kΩ

For the purpose of identifying and categorising problems in analogue circuits, the four separate test bench circuits shown in the aforementioned diagrams are taken into consideration. This is done using a machine learning technique and meta heuristic algorithm. The output voltage and current of the circuit being tested are used to extract the characteristics, which include both actual and fictitious values of frequency response.

### 3. Methodology

Figure 4 depicts the whole procedure for diagnosing defects in analogue frequency response circuits. Data processing with GWO optimisation and fault diagnosis with SVM with HHO optimisation are the two key steps in the fault detection process. Below is a discussion of the procedure' description.



#### 3.1 Data Acquisition

The circuits that will be tested in this stage must first be developed. The circuit under test (CUT) is divided into two categories: defective and fault-free CUTs. Section 2 discusses the circuits under consideration. Tables from section 2 list both the nominal values and the fault values. For data processing, the response voltage waveforms of circuits with and without faults are recorded.

#### 3.2 Processing of Data

The Sallen Key circuit has been modified by grey wolf to process the data. First, the frequency responsive curves are found, together with their peak values. Using grey wolf optimisation, features are retrieved and optimised in this stage. The circuit in Figure 5 is a generalised version of the Sallen-Key circuit where the pass-band gain is determined by R3 and R4 and generalised impedance terms, Z, are used for the passive filter components.

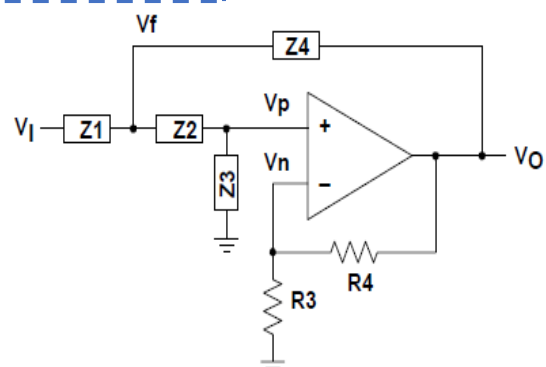


**Fig. 5 General Diagram of SKC**

KCL at  $V_f$ :

$$V_f \left( \frac{1}{Z_1} + \frac{1}{Z_2} + \frac{1}{Z_4} \right) = V_i \left( \frac{1}{Z_1} \right) + V_p \left( \frac{1}{Z_2} \right) + V_o \left( \frac{1}{Z_4} \right) \quad (1)$$

KCL at  $V_p$ :

$$V_p \left( \frac{1}{Z_2} + \frac{1}{Z_3} \right) = V_f \left( \frac{1}{Z_2} \right) \rightarrow V_f = V_p \left( 1 + \frac{Z_2}{Z_3} \right) \quad (2)$$

KCL at  $V_n$ :

$$V_n \left( \frac{1}{R3} + \frac{1}{R4} \right) = V_o \left( \frac{1}{R4} \right) \rightarrow V_n = V_o \left( \frac{R3}{R3+R4} \right) \quad (3)$$

By considering this SKC, different types of circuits are designed and the features are extracted. Some of the features are:

- amplitude with maximum peak for the output voltage response which is real.
- amplitude with minimum peak for the output voltage response which is imaginary.
- amplitude with minimum peak for the output voltage response which is imaginary.
- amplitude with maximum peak for the supply current response which is real.
- amplitude with maximal peak for the supply current response which is imaginary.
- amplitude with minimum peak for the supply current response which is imaginary.

Once this input data is arranged in matrix form—which does represent a substantial amount of data given that each designed circuit has 6 characteristics—11x100 data points are provided to grey wolf optimisation in order to reduce the number of features that are obtained for each SKC.

### Grey wolf optimization

The Grey Wolf Optimisation (GWO) algorithm imitates the strong leadership structure and hunting strategy of grey wolves. The leadership system is demonstrated using the alpha, beta, delta, and omega kinds of grey wolves. The administrative order and wolf chasing processes are modelled by this GWO calculation. The three primary processes in the

hunting process include seeking for prey, surrounding the prey, and ultimately assaulting the victim. The GWO approach is put into practise using these three stages [17]. Fig. 6 depicts the GWO process's overall flow. The prey's three vector positions are written as  $P(\alpha), P(\beta)$  and  $P(\delta)$ . Equations (4), (5), and (6) define the velocities.

The equations can be shown as:

$$V_\alpha = |C \cdot P_\alpha(t) - P(t)| \quad (4)$$

$$V_\beta = |C \cdot P_\beta(t) - P(t)| \quad (5)$$

$$V_\delta = |C \cdot P_\delta(t) - P(t)| \quad (6)$$

$V_\alpha, V_\beta$  and  $V_\delta$  are termed as the velocity of the wolf that is updated w.r.t to best position and initial position  $P(t)$  of the wolf.

The updated positions are given in eq (7), (8) (9):

$$P_1 = P_\alpha - B \cdot V_\alpha \quad (7)$$

$$P_2 = P_\beta - B \cdot V_\beta \quad (8)$$

$$P_3 = P_\delta - B \cdot V_\delta \quad (9)$$

$P_1, P_2$  and  $P_3$  are the positions of the wolfs that are updated.

The vector coefficients are termed to be B and C and are evaluated as Eq 10 and Eq 11

$$B = 2b \cdot r_1 - b \quad (10)$$

$$C = 2 \cdot r_2 \quad (11)$$

where  $r_1, r_2$  are the random forms of the vectors in  $[0, 1]$  and b elements decrease linearly from 2 to 0 throughout the course of repetitions.

The final best position of wolf is given as,

$$P(t + 1) = P_1 + P_2 + P_3 / 3 \quad (12)$$

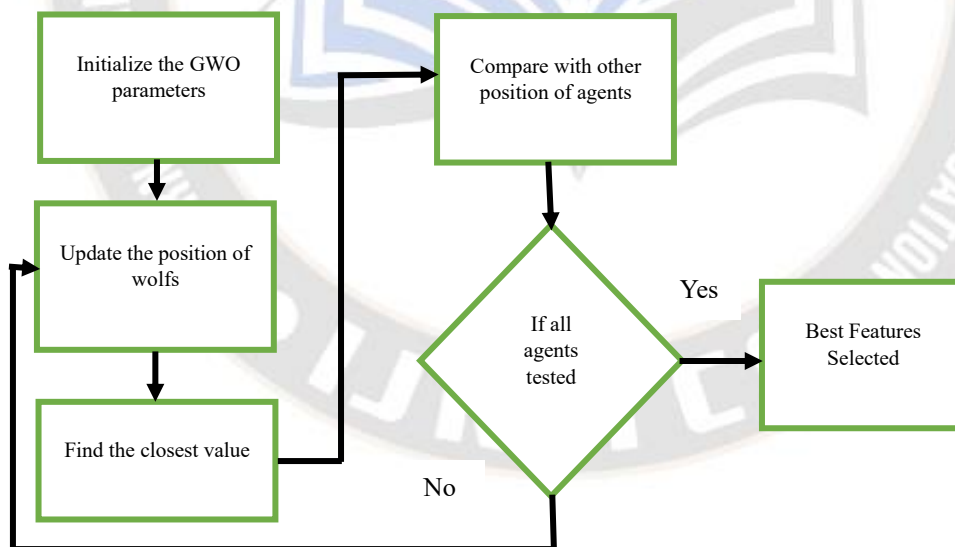


**Fig. 6 Flowchart of GWO**

The optimised classifier receives these characteristics for learning and validation. Following this round of processing, the top classifier with the highest classification accuracy was selected, which involved a reasonable number of classifiers utilising machine learning methods.

### 3.3 Support Vector Machine

In [18], the author presented the working of Support Vector Machine (SVM) [18], which was initially put out to address

the process of how the data is divided linearly i.e., binary classification and is shown in Fig.7. H1 and H2 are the two classes of planes that pass through the nearest sample points above and below the plane H and parallel to H, respectively, if H is the ideal classification hyperplane. The black and white dots indicate two classes of samples. In this analysis the terms H1 and H2 are said to be the support vectors and the separation distance between the two vectors is said to be

interval of classification. By precisely segregating the training samples at the same time, the optimal classification hyperplane H enhances the interval of classification.

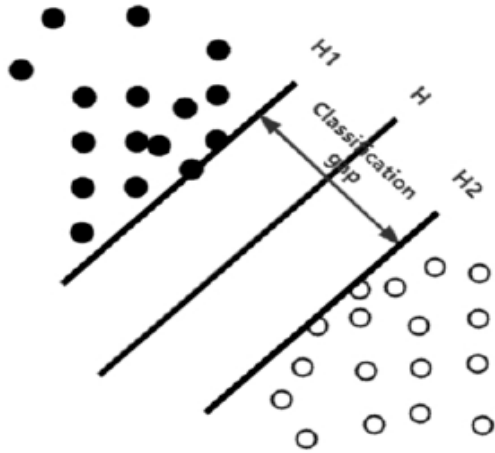


Fig. 7 Working of SVM model

The supposed set of samples for training  $(x_i, y_i)$ ,  $i = 1, 2, \dots, l$ , and the input vectors  $x_i \in R^d$ , and  $y_i \in \{-1, 1\}$  are the labels which comes under suggested category and ideal classification hyperplane 'H' formulation is as follows  $\omega^T X + b = 0$  (13)

Where  $\omega \in R^d$  is termed as the normal vector of the hyperplane which is classified and  $b \in R$  is called the threshold, while making:

$$\begin{cases} \omega^T x_i + b \geq 1, y_i = 1 \\ \omega^T x_i + b \leq -1, y_i = -1 \end{cases}; i = 1, 2, \dots, l \quad (14)$$

That is, under the constraint of  $y_i(\omega^T x_i + b) \geq 1$ , with  $\|\omega\|$  indicating the vector  $\omega$  mode, The plane H precisely determines the categorization interval as  $\frac{2}{\|\omega\|}$ , by which the interval of classification will be increased when  $\|\omega\|$  takes the minimized value. The quadratic programming optimisation task with limitations, which is translated into formula (15), that maximises the classification interval specified by the H plane for the linearly divisible situation.

$$\min_{w,b} \frac{1}{2} \|\omega\|^2 \quad s.t \quad y_i(\omega^T x_i + b) \geq 1, i = 1, 2, \dots, l \quad (15)$$

To solve the above eqn (15), a Lagrange optimization methodology is utilized and the decision function is achieved after the transformation:

$$f(x) = \text{sgn}(\sum_{i=1}^l \alpha_i y_i x_i + b) \quad 0 < \alpha_i < C \quad (16)$$

In the case of nonlinear classification, SVMs use nonlinear mapping to convert data from a low-dimensional, linearly indistinguishable space to a high-dimensional, linearly different feature space. In order to guarantee classification performance in the event of linear indistinguishability, SVM incorporates kernel functions that employ a particular function of the original space rather than the inner product of the converted space for calculation. To overcome this issue, a dimensional catastrophe in the mapped feature space can exist. With the formula (17), where  $\sigma$  is the radial basis radius, we employ a Gaussian kernel function (RBF function).

$$K(x, x_i) = \exp \left[ -\frac{|x-x_i|^2}{\sigma^2} \right] \quad (17)$$

The decision function (16) becomes equation (18) with the addition of the kernel function.

$$f(x) = \text{sgn}(\sum_{i=1}^l \alpha_i y_i K(x, x_i) + b) \quad 0 < \alpha_i < C \quad (18)$$

The decision function's (eq. 18) parameter C is a penalty factor that is used to modify the samples' misclassification rate and complexity in order to improve the classifier's generalisation capacity.

### 3.4 Harris Hawks Optimization

The suggested HHO's exploratory and exploitative stages were inspired by Harris hawks' various attacking tactics, including surprise pounces and prey exploration. Given that HHO is a population-based, gradient-free optimisation method, any optimisation issue may be addressed with it with the right formulation. When Harris' hawks hunt, they use their sharp vision to follow and locate their prey, although occasionally the prey is not readily visible. In order to discover a prey, the hawks wait, watch, and monitor the desert area. This might take many hours.

$$X(t+1) = \begin{cases} X_{rand}(t) - r_1 |X_{rand}(t) - 2r_2 X(t)| & q \geq 0.5 \\ (X_{rabbit}(t) - X_m(t)) - r_3(LB + r_4(UB - LB)) & q < 0.5 \end{cases} \quad (19)$$

The average position of hawks is attained using,

$$X_m(t) = \frac{1}{N} \sum_{i=1}^N X_i(t) \quad (20)$$

The total numbers of hawks are termed to be 'N', the position of each hawk is represented as  $X_i(t)$  during the 't' iterations.

Although there are alternative ways to determine the average location, we chose the most obvious rule. The HHO algorithm may move from exploration to exploitation and then between additional exploitative behaviours based on the energy of the escaping victim. A prey loses a lot of energy while it attempts to flee. The following prey energy model illustrates this fact:

$$E = 2E_0 \left( 1 - \frac{t}{T} \right) \quad (21)$$

where 'T' is termed as the number of repetitions to a maximum extent,  $E_0$  is the starting state of the energy, and E is the prey's fleeing energy.

### 3.5 SVM Classifier Based on HHO

The HHO approach is suggested in this research to optimise the Gaussian kernel function's kernel width parameter g and the SVM's penalty parameter c. The algorithm is known as HHO-SVM. Here is how the optimisation process is presented:

Stage1: Initialization of data. According to the cross-validation parameters, the initial data set is divided into the training set and the testing set.

Stage2: Initialization of HHO. Decide on the populations number, the total count of iterations that may be made, the variable dimension, and the search area.

Stage3: Evaluation of Fitness value. The dataset utilized for training is fed to the SVM model, and the fitness value is



determined by calculating the test set data's prediction accuracy using the current generation  $c$  and  $g$ .

Stage4: Iteration performance of Algorithm. Updates to the classifying model were made using HHO in accordance with the fitness value.

Stage5: Repeat the third and fourth phases once the number of iterations reaches the maximum number of iterations. Currently, the ideal parameters are  $c$  and  $g$ .

**4. Experimental Results**

To analyse and find defects in frequency response analogue signals (FRAS), fault and non-fault signals were constructed in this study. For this, several signals with diverse AC and DC fault types were developed. The 12 attributes that depend on the voltage, current, and each of their independent components are extracted using these signals. Some of these characteristics are improper for training, and using them would result in errors and poor detection accuracy. To do this, the best and most accurate qualities should be used. As a result, the HHO optimised SVM classifier uses the GWO Method for feature selection. The tables below display the accuracy outcomes under various fault conditions. For salient key circuits, a greater rate of accuracy was achieved utilising two optimisation techniques, one for near feature selection and the other for near classifier. With the help of suggested model the diagnosis of fault capacity need to be verified, the first example circuit is a SK-LPC followed by SK-HPC, SK-BPC and SK-BSC, which are a benchmark circuits and is used as a CUT. The results of accuracy are shown below.

**Table 5. Rate of Accuracy in identifying the fault class for SK-LPC**

Fault Class	Accuracy (%)
F4	99.4
Others	100
Average	99.963

**Table 6. SK-LPC test accuracy results**

Method	Accuracy (%)
SK-LPC with SVM	98.05
GOA – SK-LPC with SVM	98.56
SK-LPC with HHO – SVM	99.02
GOA – SK-LPC with HHO– SVM	99.96

**Table 7. Rate of Accuracy in identifying the fault class using SK-HPC**

Fault Class	Accuracy (%)
F4	99.73
Others	100
Average	99.982

**Table 8. SK-HPC test accuracy results**

Method	Accuracy (%)
SK-HPC with SVM	98.10
GOA – SK-HPC with SVM	98.45
SK-HPC with HHO – SVM	99.14
GOA – SK-HPC with HHO– SVM	99.982

**Table 9. Rate of Accuracy in identifying the fault class for SK-BPC**

Fault Class	Accuracy (%)
F5	99.32
F8	99.67
Others	100
Average	99.94

**Table 10. SK-BPC test accuracy results**

Method	Accuracy (%)
SK-BPC with SVM	98.15
GOA – SK-BPC with SVM	98.50
SK-BPC with HHO – SVM	99.22
GOA – SK-BPC with HHO– SVM	99.94

**Table 11. Rate of Accuracy in identifying the fault class for SK-BSC**

Fault Class	Accuracy (%)
F5	99.42
F8	99.65
Others	100
Average	99.945

**Table 12. SK-BSC test accuracy results**

Method	Accuracy (%)
SK-BSC with SVM	98.0
GOA – SK-BSC with SVM	98.6
SK-BSC with HHO – SVM	99.2
GOA – SK-BSC with HHO– SVM	99.945



The aforementioned data demonstrate that among the CUTs taken into consideration, the suggested HHO-SVM outperforms all other comparison algorithms for all salient key circuits, demonstrating HHO's potent optimisation capabilities. To further understand the convergence performance of HHO, three example methods from each benchmark category are individually computed to solve the convergence curves as shown in Figure 8. The results are listed as  $f_3$ ,  $f_4$ ,  $f_7$  and  $f_9$ .

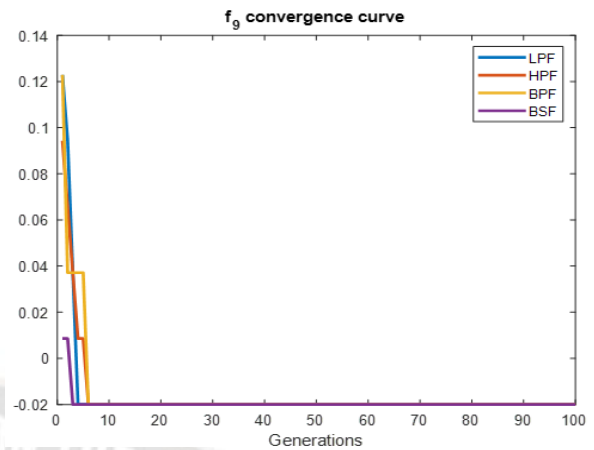
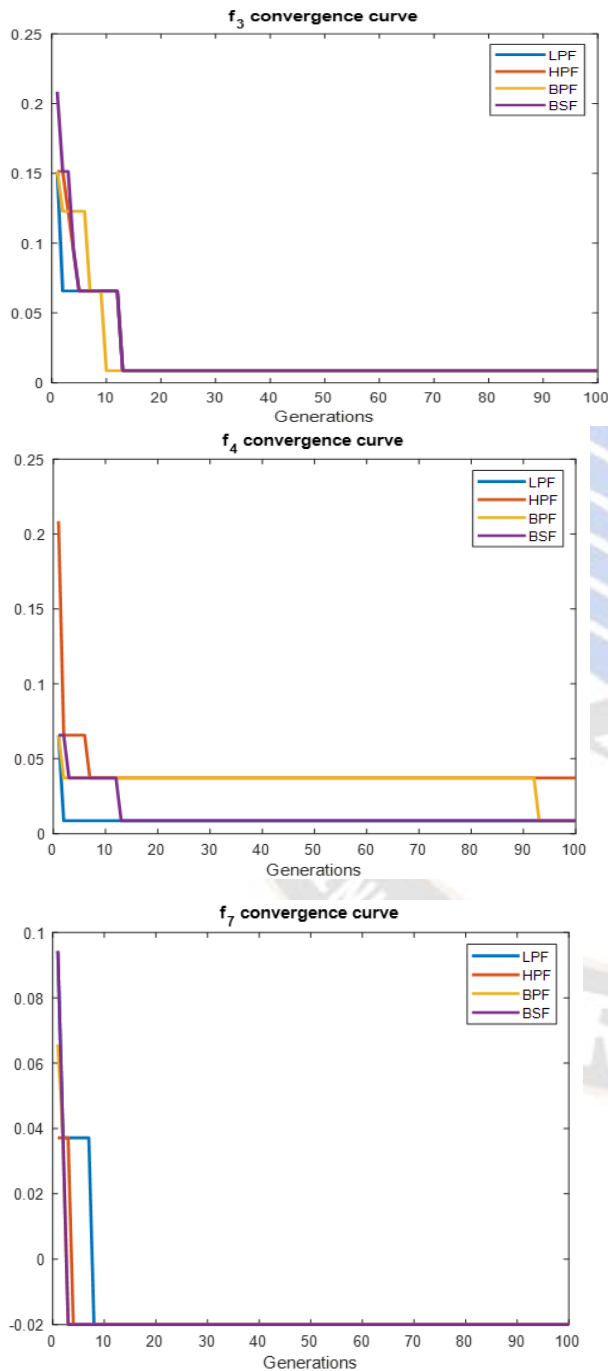


Fig. 8 Comparison of convergence curve of different Sallen key circuits

### 5. Conclusion

In the research that was just presented, a methodology for identifying and categorising errors that influence frequency response analogue integrated circuits was introduced. The MATLAB program's machine learning and optimisation algorithms for fault categorization provide the foundation for this. This study presents an effective technique for diagnosing analogue circuit faults. The suggested method's two main steps, the first of which is the extraction of optimised features and the second of which is classification based on an optimisation strategy, are its key contributions. The performance of the SVM classifier is evaluated, and an HHO approach is suggested to improve it. Test results demonstrate that the HHO method can efficiently increase the accuracy of classification and the efficiency of SVM parameter optimisation. When the fault parameters are distributed and created using a two-end optimisation model, the suggested fault diagnostic method has a 99.95% accuracy rate, which is 1.9% greater than methods that do not employ the optimisation process. The accuracy rate achieved for the corrected fault parameter is 100% by using the suggested method.

### Conflicts of Interest

The authors declare no conflict of interest

### Acknowledgment

R. Gurunadha conducted the research work, collected the data, and wrote the paper. Dr. K. Babulu supervised the work and approved the final version.

### References

- [1] M. Parai, S. Srimani, K. Ghosh, H. Rahaman, "Multi-source data fusion technique for parametric fault diagnosis in analog circuits," *Integration: VLSI, J.* 92 (2022) 92–101.
- [2] A. Arabi, N. Bourouba, N. Belaout, M. Ayad, "An accurate classifier based on adaptive neuro-fuzzy and feature selection techniques for fault classification in analog circuits," *Integration: the VLSI J.* 64 (2019) 50–59.

- [3] I. Laidani, N. Bourouba, Analog Circuit Fault Classification and Data Reduction Using PCA-ANFIS Technique Aided by K-means Clustering Approach,” *Adv. Electrical Comput. Eng.* 22 (4) (2022) 73–82.
- [4] M. Parai, S. Srimani, K. Ghosh, H. Rahaman, “Analog Circuit Fault Detection by Impulse Response-Based Signature Analysis,” *Circuits, Syst., Signal Process.* 39 (2020) 4281–4296.
- [5] T. Gao, J. Yang, S. Jiang, C. Yang, “A novel fault diagnostic method for analog circuits using frequency response features,” *Rev. Sci. Instrum.* 90 (10) (2019) 104708.
- [6] B.A. Abo-elftooh, M.H. El-Mahlawy, H.F. Ragai, “New digital testing for parametric fault detection in analog circuits using classified frequency-bands and efficient test-point selection,” *Ain Shams Eng. J.* 12 (2021) 1701–1721.
- [7] B. Esen, A. Coyette, G. Gielen, W. Dobbelaere, R. Vanhooren, “Effective DC fault models and testing approach for open defects in analog circuits,” *IEEE International Test Conference (ITC)*, 2016, pp. 1–9.
- [8] M. Merabet, N. Bourouba, “DC Hard Faults Detection and Localization in Analog Circuits Using Fuzzy Logic Techniques,” *Electron. J.* 23 (1) (2019) 18–25.
- [9] M. Tadeusiewicz, S. Hałgas, “A method for multiple soft fault diagnosis of linear analog circuits,” *Measurement* 131 (2019) 714–722.
- [10] L. Nguyen, “Tutorial on Support Vector Machine”, Special Issue – Novel Algorithms for Global Optimization and Relevant Subjects”. *Appl. Comput. Math.* 2016, 6, 1–15.
- [11] J. Du, Y. Liu, Y. Yu, W. Yan, “A Prediction of Precipitation Data Based on Support Vector Machine and Particle Swarm Optimization (PSO-SVM),” *Algorithms* 2017, 10, 57.
- [12] S. Khozani, “Application of a Genetic Algorithm in Predicting the Percentage of Shear Force Carried by Walls in Smooth Rectangular Channels.” *Meas. J. Int. Meas. Confed.* 2016, 87, 87–98.
- [13] R. Eberhart, J. Kennedy, “A New Optimizer Using Particle Swarm Theory,” In *Proceedings of the International Symposium on Micro Machine and Human Science*, Nagoya, Japan, 4–6 October 1995; pp. 39–43.
- [14] S. Mirjalili, “The Ant Lion Optimizer,” *Adv. Eng. Softw.* 2015, 83, 80–98.
- [15] D.H. Wolpert, W.G. Macready, “No Free Lunch Theorems for Optimization.” *IEEE Trans. Evol. Comput.* 1997, 1, 67–82.
- [16] M.H. Sulaiman, Z. Mustaffa, M.M Saari, H. Daniyal, Barnacles, “Mating Optimizer: A New Bio-inspired Algorithm for Solving Engineering Optimization Problems,” *Eng. Appl. Artif. Intell.* 2020, 87, 103330.
- [17] S. Mirjalili, S.M. Mirjalili, A. Lewis, “Grey Wolf Optimizer,” *Adv. Eng. Softw.* 2014, 69, 46–61.
- [18] V.N. Vapnik. “*Statistical Learning Theory*,” John Siley and Sons, 1998.